Asian Journal of Chemistry; Vol. 34, No. 6 (2022), 1581-1586

ASIAN JOURNAL OF CHEMISTRY

https://doi.org/10.14233/ajchem.2022.23623

Equatorial Gate Opening Efficiency of Single and Double, S-S Gated Hemicarcerands

GAYATHRI SANKAR

Department of Chemistry, Mahatma Gandhi College (Affiliated to University of Kerala), Thiruvananthapuram-695004, India

Corresponding author: E-mail: gayathrisankar009@gmail.com

Received: 16 November 2021; *Accepted*: 17 April 2022; *Published online*: 18 May 2022; AJC-20826

Covalent disulphides bonds are very strong in oxidizing environments and are weakened in reducing environments. So far, there has been no reported study on multi-gate induced hemicarcerands. In this work, the stability and redox properties were investigated, as well as efficiency of the number of disulphide gates can provide in equatorial escape of a guest in two chosen hemicarcerand systems. Single and opposite double gated hemicarcerands were designed in Gauss view 5.0 and structures were optimized using HF 3-21G* basis set. It is concluded from the studies that the opposite double gated system has more guest encapsulating efficiency in redox conditions than single gated hemicarcerand, which makes it a potential cancer drug carrier due to its selective gate opening at high redox conditions.

Keywords: Encapsulation efficiency, Hemicarcerand, Multi-gated, S-S gate.

INTRODUCTION

Molecular jails or carcerands were first described by Donald J. Cram, as a host molecule that completely entrapped its guest, so that it could not escape even under high temperatures [1]. In contrast for hemicarcerands, though it allowed guests to form stable complexes at ambient temperatures, at high temperatures it opened and closed for guest entry and exit. The interior of the host molecule was described as the new phase of matter by Cram, in which radically different reactivity was observed. Several researchers [2,3] stabilized and characterized many highly reactive intermediates such as anti-aromatic cyclobutadiene, benzyne, carbenes and nitrenes, on complexation with the host. The cavities are suitable for a large number of guests irrespective of size, shape and phase of matter, ranging from Xe [2] gas to C_{60} [4] fullerene solid. The inside of an eight-hemicarcerand agglomerated structure can be as large as 1700 Å [5].

The molecular mechanics calculations by Nakamura showed results of change in conformation in the hemicarcerand on increasing temperature that decreased constrictive binding, which hence gave way for guest escape. The decrease in constrictive binding was due to conformational change of the bridges of the hemicarcerands from chair to boat, making an opening for the guest to leave the cavity. The phenomenon was studied by Chapman & Sherman who named the chair and boat conformational bridged hemicarcerands as wrapped and unwrapped hemicarcerands [6,7]. They introduced the term twistomers to the two twisted enantiomers. Twistomerism showcased by hemicarcerand made a possible way of equatorial escape for the guest molecule.

The concept of Gating was put forth to look into the possibilities of designing controllable passages for guests to enter and leave the host cavity. Gates could be implemented according to the need of mechanism of its opening. The mechanism to be opted in a gating depends upon the guest size and shape. Later, studies were conducted on redox and photochemical stimulus on hemicarcerand systems reported by Houk *et al.* [8] using molecular mechanics-computational method and corresponding experimental work. Houk designed a hemicarcerand bearing a single disulphide-dithiol redox-controllable gate and made it complex with seven guests. Three guests, out of the seven formed stable host-guest complexes, which were observed from H^1 NMR spectra. Three stable complexes formed were studied under reducing conditions. Gate-opening and guest-release was found accelerated as reducing strength in the environment increased [8].

The disulphide bond consists of two sulphur atoms sharing a symmetric bond with its lone pairs. The RS-SR bond molecular bonding (M.O.) calculations yield that they form filled

π and π* molecular orbitals [9]. Addition of an electron to such a system can only accommodate it in its π* molecular orbital. The energy of this molecular orbital is very high and has high anti-bonding character, leading the molecule induced with a disulphide bond to open up. Hence, the disulphide linkages are particularly amenable to reduction, leading to bond weakening. Fig. 1 represents opening of S-S bond on reduction.

However, Houk's work [8] was confined to the area of having just one single disulphide-dithiol gate induced to a typical hemicarcerand, and the reason for opening of gate was not qualitatively explained. Sherman *et al*. [10] had reported a hemicarcerand with four disulphide bridges which claimed to perform guest exchange under redox conditions. There is no reported study on multi-gate induced hemicarcerands. A comparative study is yet to be done on efficiency, the number of disulphide gates can provide in paving way for equatorial escape of a guest. The number of disulphide bridge arrangements possible for a typical four bridge hemicarcerand is shown below. Two disulphide gate-induced hemicarcerand can have the disulphide bridges at opposite positions or at adjacent positions, which make the number of arrangements of disulphide gates five (Fig. 1b). The larger the guest, the wider the exit has to be, the more number of gates that has to open up is the assumption when it comes to the application phase.

In this work, the stability and redox properties are studied, as well as efficiency; the number of disulphide gates can provide in equatorial escape of a guest in a hemicarcerand system with two of the stated possibilities. A comparative study of efficiency of both chosen hemicarcerands is done using HF 3-21G* basis set in Gaussian 0.9 [11]. We also put forward an explanation on basis of molecular orbital calculations, for gate opening in disulphide gate induced hemicarcerands. The main application of this host system when induced with disulphide bonds will be in the field of drug delivery. Cancer cells were compared to normal cells produce two to five times the concen-tration of glutathione (GSH) [12]. The main group in glutathione being thiol, the high thiol concentration opens the gate of disulphide gate induced hemicarcerand more rapidly at the cancer cell site than at the normal cell site. This gives hope for a very target specific drug carrier in case of cancer treatment.

EXPERIMENTAL

Gauss View 5.0 was used for visualization and designing of the molecule under study. Gussian09 was used to optimize and study molecular orbital calculations, under cluster computing with 8 processors.

Theoretical background

Self-consistent field method: The self-consistent procedure is carried out to evaluate the orbital coefficients from this to arrive at the best solution. The self-consistent field (SCF) [13,14] is used in quantum mechanics that give the best descri-

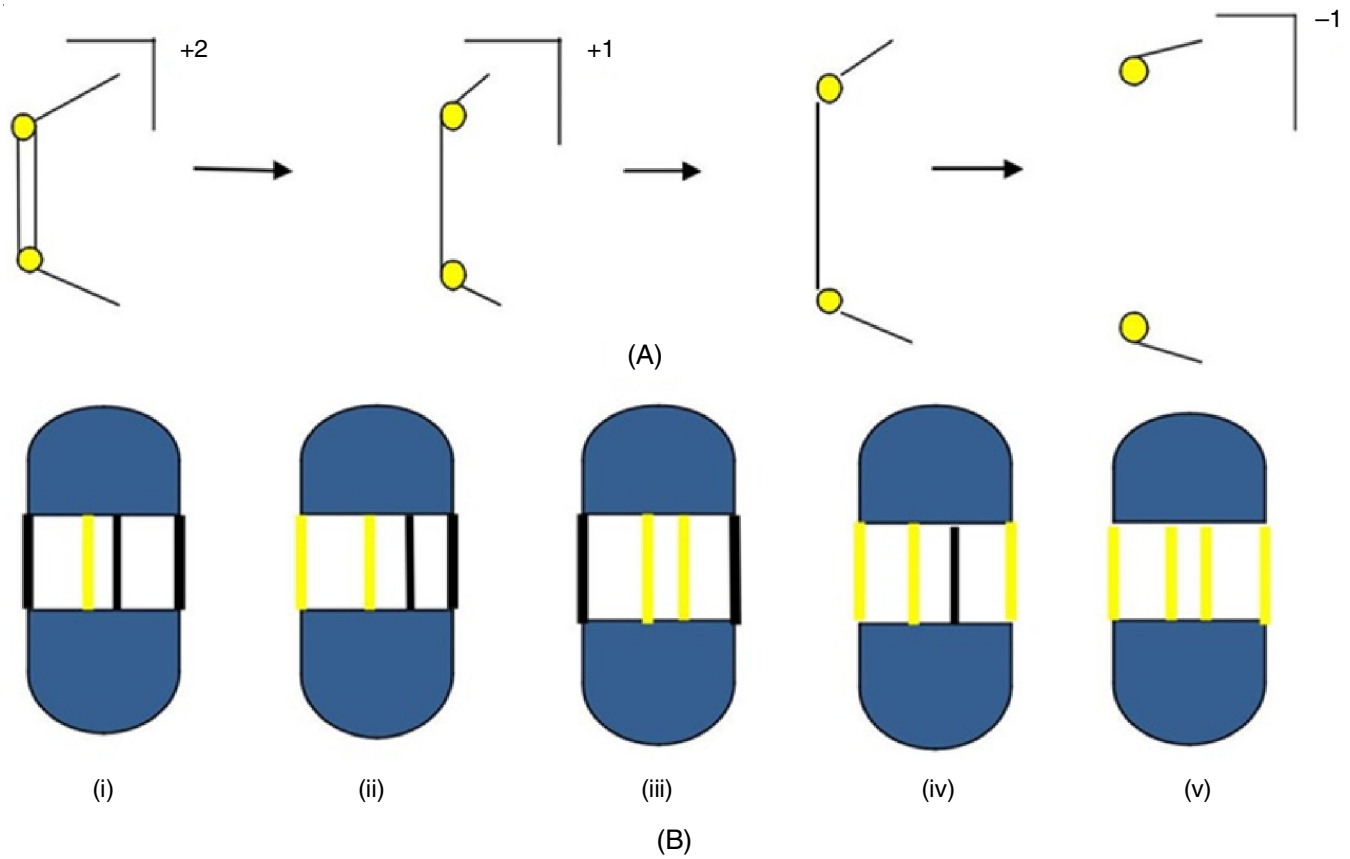

Fig. 1. (a) The increase in bond length between the two sulphur atoms is shown as the charge changes from +2 to -1. (b) Hemicarcerand induced with (i) Single disulphide gate, as in Houk's work. (ii) Two disulphide gates at adjacent positions (iii) two disulphide gates opposite to each other (iv) Three disulphide gates (v) All four disulphide gates. The yellow lines denote bridges induced with disulphide gate

ption of the electronic wave function of a system in terms of minimal number of anti-symmetrized product of one electron function. A schematic representation of the procedure is shown in Fig. 2.

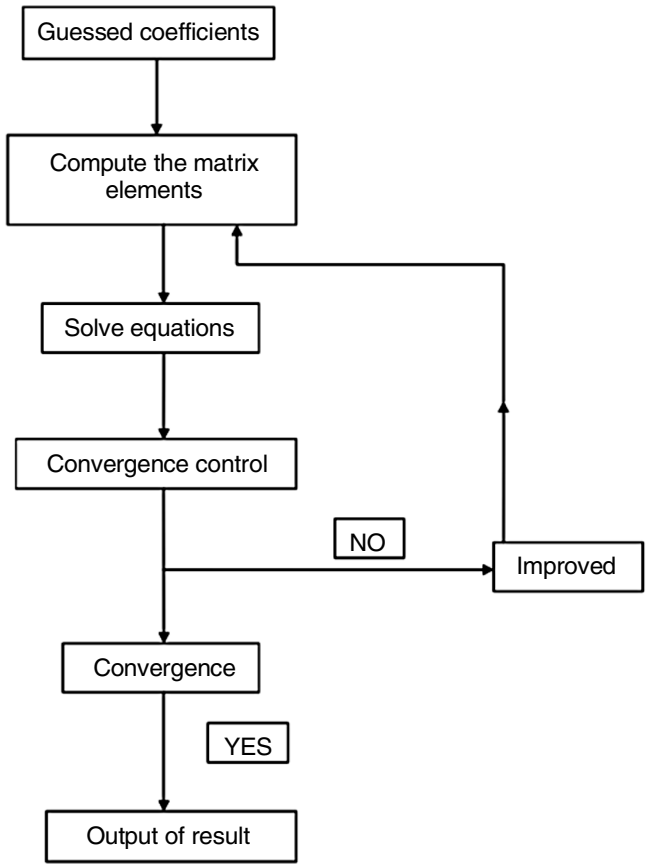

Fig. 2. Schematic representation of SCF procedure

First step is the construction of a trial function, for that a Slater determinant [15] must be constructed. It is more usual to start with a more realistic guess so as to reduce the number of SCF iterations. Diagonalization and suitable reordering usually in terms of energy give improved expansion coefficients. This is first cycle of SCF procedure. The second and subsequent cycles proceed as above and improved coefficients are generated by the previous iteration. An alternative procedure leading to equivalent result is to construct the operator on the basis of the trial molecular orbitals, rather than on the basis of the atomic orbital.

Hatree-Fock method: Simplest *ab initio* [16] calculation is a Hatree-Fock [9,17] calculation. The problem which Hatree addressed raised from the fact that for any atom with more than one electron, an exact analytical solution of Schrodinger equation is not possible, because of $e^- - e^-$ repulsion term. Hatree's method approximates poly-electronic wave function for an atom as product of many e^- functions.

$$\psi_0 = \psi_{0(1)}\psi_{0(2)}\psi_{0(3)} \ldots\ldots\ldots\ldots\psi_{0(n)}$$

The function is called a Hatree product, where, $\psi_{0(1)}$ is the poly electronic wave function of an atom. $\psi_{0(1)}$ is the function coordinates of e^-1 of an atom. $\psi_{0(2)}$ is the function coordinates of e^-2 of an atom. $\psi_{0(1)}$, $\psi_{0(2)}$, $\psi_{0(3)}$ ..... $\psi_{0(n)}$ are atomic orbitals. ψ_k, for k cycles, if wave function is same as the wave function from the previous cycle (k-1), it can be said that the field is consistent to the previous field and Hatree method is called SCF.

Hatree-Fock method in cooperates anti-symmetrized product of one e^- wave function of Slater determinant. Hatree wave function is a product of one e^- function called spatial orbitals, but slater orbitals are composed of spin orbitals. Hatree-Fock calculations hence take into account both spatial and spin content for orbitals.

Energy calculation for atomic or molecular energy is done using the equation given below:

$$E = \frac{\int \psi^* A \psi d\tau}{\int \psi^* \psi d\tau}$$

According to variation theorem, energy calculated using above equation must be greater than or equal to true ground state of the molecule.

Ab initio calculations are done using Roothan-Halls [18] eqn.:

$$\sum_{s=1}^{m} F_{rs}C_{si} = \sum_{s=1}^{m} S_{rs}C_{si}E_i$$

r = 1, 2, 3, ….m for each i = 1, 2, 3, ….m.

Post Hatree-Fock calculations include a phenomenon called e- correlation, where motions of pair of electrons in atoms or molecules are connected. Due to this $e^- - e^-$ repulsion becomes smaller than that predicted by Hatree-Fock method. Electronic energy is hence lower than predicted. Thus main defect of Hatree-Fock is that it does not treat e^- correlation, each e^- is considered to move in an electrostatic field represented by the average positions of other electrons, where as in fact electrons avoids each other better than model predicts.

Basis set: The set of functions called basis sets [19] when combined in linear combination creates molecular orbitals.

$$\psi = c_1\phi_1 + c_2\phi_2$$

where ϕ_1 and ϕ_2 are basis functions of an atom and c_1 and c_2 are weighing coefficients to get best ψ.

For many number of molecules, the equation used is:

$$\psi i = \sum_{s=1}^{m} C_{si}\phi_s$$

where ψi is the i^{th} molecular orbital.

These functions are either Slater type orbitals (STOs) or Gaussian type orbitals (GTOs). The STOs are difficult to calculate and mainly used for atomic and diatomic systems, where high accuracy is required and also used partly in DFT method. The STOs can be approximated by linear combination of GTOs. Easier calculation of overlap and other integrals with Gaussian basis function leads to huge computational savings [20]. In this work, we have used a combination of polarized and Pople basis sets [21], where polarized basis set considers distortion in shape of the atomic orbital to be due to coming together of atoms that causes a polarization effect. It takes into account the small *d*-character *p*-orbital poses and small *p*-character s orbital poses. Pople basis set comes with a notation X-YZG. As inner electrons are not as vital as valance e^- for calculation,

they are described as a single Slater orbital and double zeta is calculated only for the valance electrons. Double zeta calculation is where each atomic orbital is taken as a linear combination of STOs differing in effective nuclear charge.

RESULTS AND DISCUSSION

The CIF file for the molecules chosen for study was not obtained, hence they were designed. Design of the Container head molecule: The container head was designed in Gauss view 5.0 and optimised using HF/3-21G* basis set. The optimized container head was of C_2 symmetry.

Opposite double-gated hemicarcerand: The opposite double-gated hemicarcerand was constructed in Gauss view 5.0 by linking two container heads with (-CH_2-S-S-CH_2-) at the flattened faces. The reason of giving this linker group at the flattened faces, since it was the best possibility to get a symmetric hemicarcerand. The edged faces were then connected by (-CH_2)$_5$ linkers. The reason for using five CH_2 groups as linkers was because it was the least number of CH_2 groups that were required to form a closed hemicarcerand. The molecule of hemicarcerand thus designed was the smallest, which could be designed with a stable structure and also the minimal number of atoms. The designed structure had Cs symmetry and was optimized using HF/3-21G* basis set, to yield an optimized structure with C1 symmetry. The optimized structure had the S-S bond lengths as shown in Table-1. The optimized figures showed benzene rings with all double bond, this may be due to the basis set employed and the limitation of bond length cut offs implemented in the visualisation software.

The disulphide linkages are particularly amenable to reduction, leading to the bond weakening. The anion radical of corresponding double gated structures were optimized using HF/3-21G* level of theory, to study the disulphide-gate opening mechanism. It is expected that both the gates would open upon reduction, but the result was contradicting. Only a single gate was opened in the anionic structure as in Fig. 3a. The dianion

TABLE-1
TABLE OF CHARGE, MULTIPLICITY AND BOND LENGTH OF THE OPPOSITE DOUBLE GATED HEMICARCERAND

Type of molecule	Charge	Multiplicity	S-S bond length of gate (i) [Å]	S-S bond length of gate (ii) [Å]
Neutral hemicarcerand with opposite double-gates	0	1	2.054	2.054
Hemicarcerand anion with opposite double-gates	-1	2	2.820	2.056
Hemicarcerand anion with opposite double-gates	-2	1	5.653	2.057

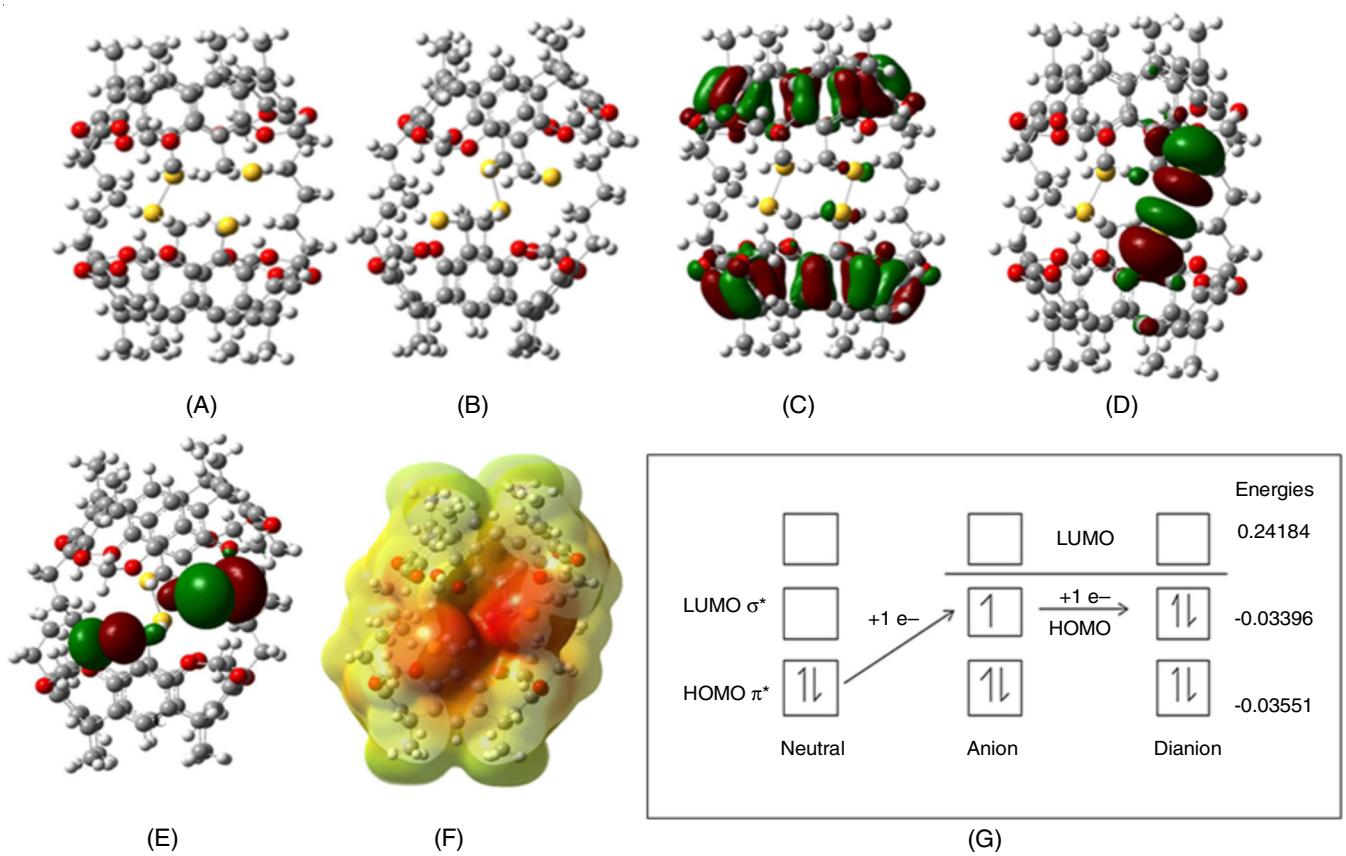

Fig. 3. (a) Optimized anion radical of opposite disulphide-gated hemicarcerand, (b) Optimised dianion opposite disulphide gated hemicarcerand, (c to e) Depicts M.Os of molecules (c) neutral hemicarcerand, (d) Anion molecule having antibonding character, (e) Dianion molecule having very high anti bonding character, further separating gates, (f) depicts ESP visualised output of dianion molecule, which shows high electron concentration on the dianion disulphide gate owing to repulsion (g) Schematics showing the change of HOMO of molecule as e^-s are added

as in Fig. 3b showed only a further relaxation in the already opened disulphide gate and the other gate was seen to be still intact. The dianionic structure is also seen to have some structural distortions from that of the neutral structure. The explanation for this unexpected behaviour is put forth in this work using molecular orbital calculations. The HOMO of the neutral molecule (Fig. 3c) has no contribution from sulphur atoms while the LUMO has anti-bonding contribution from one of the S-S gate. The HOMO of the anion radical is the LUMO of the neutral molecule (Fig. 3g), which has an anti-bonding π character, in short the contributing disulphide-gate constitutes the π* M.O. of the molecule. There is no contribution of sulphur atoms of the other disulphide-gate. In other words, in the anion, the extra added electron entered into the LUMO of the neutral molecule and became the HOMO of the anion. The M.O. visualization (Fig. 3d) accounts that the HOMO of the anion, where the extra electron enters, with preference to the neutral molecule, has an anti-bonding σ character (σ*). The increased anti-bonding character of the contributing disulphide gate, brings about the relaxation in bond length and hence the gate opening.

The M.O. visualization (Fig. 3e) indicates that the HOMO of the dianion molecule has anti-bonding σ character (σ*). The structural changes seen in dianion molecule can be explained on the basis of ESP calculations. The high electron density on the two sulphur atoms in the opened gate is the reason for highly parted orientation of the sulphurs in the dianion structure, as indicated by the ESP visualisation (Fig. 3f).

Single-gated hemicarcerand: Houk's work [8] did not provide the satisfactory explanation regarding the reason for gate opening in single gated hemicarcerands, and so herein we try to explain it with the help of M.O. calculations using HF/3-21G* level theory. The single gate hemicarcerand designed in GaussView 5.0.9 was optimized. The optimized structure (Fig. 4a) had the S-S bond lengths as shown in Table-2.

The M.O. visualisation of the neutral molecule showed that the S-S bonds contributed very small anti-bonding character, as shown in Fig. 4c. The disulphide linkages are particularly amenable to reduction, leading to the bond weakening. The anion radical of corresponding double gated structures were optimised using HF/3-21G* level of theory, to study the disul-

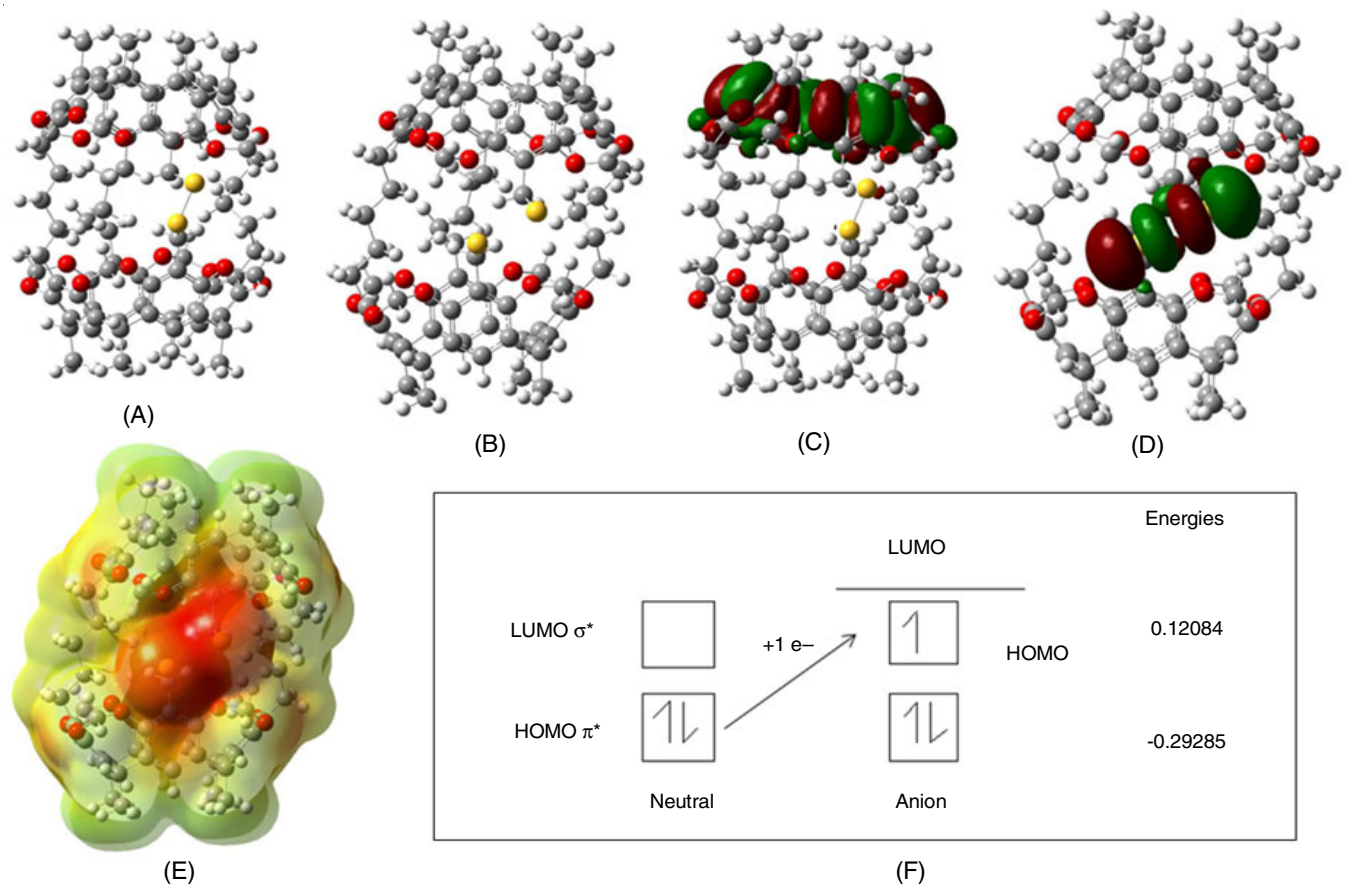

Fig. 4. (a) Optimised single gated hemicarcerand, (b) single gated anion (c) M.O visualisation of neutral single gated molecule (d) M.O visualisation of single gated anion (e) depicts ESP visualised output of anion molecule, (f) Scheme showing the change of HOMO of molecule as e^-s are added

TABLE-2
TABLE FOR CHARGE, MULTIPLICITY AND BOND LENGTH OF THE SINGLE GATED HEMICARCERAND

Type of hemicarcerand	Charge	Multiplicity	S-S bond length (Å)
Single gated neutral emicarcerand	0	1	2.056
Single gated hemicarcerand anion	-1	2	5.653

TABLE-3
CALCULATION OF REDOX POTENTIAL FOR SINGLE AND DOUBLE GATED HEMICARCERANDS

Name of system	Energy of neutral molecule (KJ/mol)	Energy of anion radical (KJ/mol)	Redox potential = E (anion) – E (neutral) (eV)
Single gated hemicarcerand	-5384.347	-5384.353	6.2×10^{-8}
Opposite double gated hemicarcerand	-6059.317	-6059.325	8.2×10^{-8}

phide-gate opening mechanism. The anion as in Fig. 4b, showed an opening of the disulphide gate and also showed some structural distortions from that of the neutral structure. In the anion, the extra added electron entered into the LUMO of the neutral molecule, and became the HOMO of the anion (Fig. 4f). The M.O. visualization (Fig. 4d) accounts that the HOMO of the anion, where the extra electron enters, with preference to the neutral molecule, has an antibonding σ character (σ*). The high antibonding character of the disulphide gate, brings about the relaxation in bond length and hence the gate opening. The structural changes seen in anion molecule can be explained on basis of ESP calculations. The high electron density on the two sulphur atoms in the gate is the reason for highly parted orientation of the sulphurs in the anion structure, as accounted by the ESP visualisation (Fig. 4e).

Comparative study of the equatorial gate opening efficiency of single-gated and opposite double-gated hemicarcerands: Both the single gated hemicarcerand anion and opposite double gated hemicarcerand dianion shows the resemblance in (i) bond length between the opened gate-sulphur atoms; and (ii) a structural distortion in comparison with the corresponding neutral molecules.

From the values in Tables 1 and 2, it can be noted that efficiency of gate opening under redox condition is more for single gated hemicarcerand, as a relaxation of bond length from 2.056 Å to 5.653 Å is achieved with addition of a single e^- to the neutral molecule. The opposite double gated hemicarcerand was found to have the same efficiency of gate opening in terms of bond length, only when the molecule was converted to a dianion by abstraction of $2e^-$s and only one gate was opened. The -S-S- bond length of the gate, which opened in the neutral molecule was 2.054 Å. This underwent relaxation to 2.820 Å on addition of an e^-. Further relaxation to 5.653 Å resulted on making the molecule a dianion. The redox potential calculation is done for both systems and given below in Table-3.

Thus, we can say that single gated hemicarcerand is more effective in equatorial guest escape under redox conditions in comparison with opposite double gated hemicarcerand.

Conclusion

A typical hemicarcerand was constructed using Gauss View 5.0 and induced with a single disulphide gate and opposite double disulphide gate. Both molecules were subjected to optimization as their neutral and anionic moiety. The opposite-double gated hemicarcerand was subjected to optimisation as its dianion as well. From the results, it is evident that the opposite double gated hemicarcerand has much more effective guest encapsulating efficiency under redox conditions. We can further make a conclusion from what is observed that increasing the number of disulphide gates in the hemicarcerand would allow us to have a more controlled release of encapsulated guest under redox conditions. Selective guest release under such conditions is favourable to use the molecule as a cancer drug carrier.

ACKNOWLEDGEMENTS

The author thanks Department of Chemistry, University of Kerala, for supporting and providing the necessary infrastructure for this work.

CONFLICT OF INTEREST

The authors declare that there is no conflict of interests regarding the publication of this article.

REFERENCES

1. D.J. Cram, S. Karbach, Y.H. Kim, L. Baczynskyj and G.W. Kallemeyn, *J. Am. Chem. Soc.*, **107**, 2575 (1985); https://doi.org/10.1021/ja00294a076
2. D.J. Cram, M.E. Tanner and R. Thomas, *Angew. Chem. Int. Ed.*, **30**, 1024 (1991); https://doi.org/10.1002/anie.199110241
3. R. Warmuth and J. Yoon, *Acc. Chem. Res.*, **34**, 95 (2001); https://doi.org/10.1021/ar980082k
4. C. Vondem Bussche-Hünnefeld, D. Bühring, C.B. Knobler and D.J. Cram, *J. Chem. Soc. Chem. Commun.*, 1085 (1995); https://doi.org/10.1039/C39950001085
5. X. Liu, Y. Liu, G. Li and R. Warmuth, *Angew. Chem.*, **118**, 915 (2006); https://doi.org/10.1002/ange.200504049
6. K. Paek, H. Ihm, S. Yun and H.C. Lee, *Tetrahedron Lett.*, **40**, 8905 (1999); https://doi.org/10.1016/S0040-4039(99)01928-0
7. J.P. Snyder and L. Carlsen, *J. Am. Chem. Soc.*, **99**, 2931 (1977); https://doi.org/10.1021/ja00451a014
8. F. Liu, R.C. Helgeson and K.N. Houk, *Acc. Chem. Res.*, **47**, 2168 (2014); https://doi.org/10.1021/ar5001296
9. C.F. Fischer, Hartree-Fock Method for Atoms. A Numerical Approach, John Wiley & Sons (1977).
10. J. Sun, B.O. Patrick and J.C. Sherman, *Tetrahedron*, **65**, 7296 (2009); https://doi.org/10.1016/j.tet.2008.11.110
11. B. Nagy and F. Jensen, *Rev. Comput. Chem.*, **30**, 93 (2017); https://doi.org/10.1002/9781119356059.ch3
12. D.W. Siemann and K.L. Beyers, *Br. J. Cancer*, **68**, 1071 (1993); https://doi.org/10.1038/bjc.1993.484
13. H. Ehrenreich and M.H. Cohen, *Phys. Rev.*, **115**, 786 (1959); https://doi.org/10.1103/PhysRev.115.786
14. D.A. Liberman, D.T. Cromer and J.T. Waber, *Comput. Phys. Commun.*, **2**, 107 (1971); https://doi.org/10.1016/0010-4655(71)90020-8
15. J.C. Slater, *Phys. Rev.*, **91**, 528 (1953); https://doi.org/10.1103/PhysRev.91.528
16. M.T. Yin and M.L. Cohen, *Phys. Rev. B Condens. Matter*, **25**, 7403 (1982); https://doi.org/10.1103/PhysRevB.25.7403
17. J.C. Slater, *Phys. Rev.*, **81**, 385 (1951); https://doi.org/10.1103/PhysRev.81.385
18. X. Hu and W. Yang, *J. Chem. Phys.*, **132**, 054109 (2010); https://doi.org/10.1063/1.3304922
19. E.R. Davidson and D. Feller, *Chem. Rev.*, **86**, 681 (1986); https://doi.org/10.1021/cr00074a002
20. A.L. Magalhães, *J. Chem. Educ.*, **91**, 2124 (2014); https://doi.org/10.1021/ed500437a
21. R. Krishnan, J.S. Binkley, R. Seeger and J.A. Pople, *J. Chem. Phys.*, **72**, 650 (1980); https://doi.org/10.1063/1.438955